Continental Shelf Research 31 (2011) 939–950

Contents lists available at ScienceDirect

Continental Shelf Research

journal homepage: www.elsevier.com/locate/csr

Research papers

Hydrographic variability on a coastal shelf directly influenced by estuarine outflow

Brian Dzwonkowski [a], Kyeong Park [a,b,*], Ho Kyung Ha [b,1], William M. Graham [a,b], Frank J. Hernandez [a], Sean P. Powers [a,b]

[a] Dauphin Island Sea Lab, 101 Bienville Blvd., Dauphin Island, AL 36528, USA
[b] Department of Marine Sciences, University of South Alabama, Dauphin Island Sea Lab, 101 Bienville Blvd., Dauphin Island, AL 36528, USA

ARTICLE INFO

Article history:
Received 29 September 2010
Received in revised form
28 February 2011
Accepted 3 March 2011
Available online 16 March 2011

Keywords:
Temperature
Salinity
Sub-tidal variability
Alabama shelf
Mobile Bay
Gulf of Mexico

ABSTRACT

Hydrographic variability on the Alabama shelf just outside of Mobile Bay, a major source of river discharge into the Gulf of Mexico, is examined using time series of water column temperature and surface and bottom salinity from a mooring site with a depth of 20 m in conjunction with a series of across-shelf CTD surveys. The time series data show variability in a range of time scales. The density variation is affected by both salinity and temperature, with its relatively strong annual signal mostly determined by temperature and its year to year variability mostly determined by salinity. Seasonal mean structures of temperature, salinity, and density show a transition from estuarine to shelf conditions in which three regions with distinct seasonal characteristics in their horizontal and vertical gradient structures are identified. Correlation analysis with the available forcing functions demonstrates the influence of Mobile Bay on the variability at the mooring site. At low frequencies, river discharge from Mobile Bay has a varying influence on salinity, which is absent during the periods with unusually low discharge. At shorter synoptic time scales, both the estuarine response to the across-shelf wind stress and the shelf response to the along-shelf wind stress are significantly correlated with temperature/salinity variability: the former becoming important for the surface layer during winter whereas the latter for the bottom layer during both winter and summer. These forcing functions are important players in determining the estuarine–shelf exchange, which in turn is found to contribute to the shelf hydrographic structure.

1. Introduction

Variability in shelf hydrography occurs over a wide range of temporal and spatial scales and can result from a number of processes such as local heating/cooling at the sea surface, the introduction of fresh water from rivers and estuaries, or the imposition of oceanic/shelf slope characteristics from impinging deep sea processes. The spatial and temporal variability of temperature and salinity on a shelf is a critical component in many physical and biological processes impacting the coastal marine environment. Physically, these two properties affect water column density, whose vertical and horizontal gradients influence, and in some cases control, coastal circulation, and mixing. Sanders and Garvine (2001) noted that 'buoyancy discharge is a major forcing agent on continental shelves often dominating circulation at intermediate scales (>100 km).' Stratification, in addition to controlling shelf mixing, has been shown to promote across-shelf transport resulting from wind-driven coastal Ekman circulation (Lentz, 2001; Weisberg et al., 2001; Kirincich et al., 2005).

The timing and magnitude of stratification has long been recognized as a key driver of biological productivity in the sea. Foremost was the development of the 'Critical Depth Model,' first proposed by Sverdrup (1953). Later, the concept of stratified ocean production was used to explain enhanced fisheries recruitment (Cushing, 1990) and fine-scale distributions of zooplankton within highly stratified water columns (Bochdansky and Bollens, 2009). In addition, it is hypothesized that seasonal stratification will be greatly influenced by warming ocean trends resulting in modified ecology within plankton communities (Mackas et al., 2007).

Given the importance of understanding the temperature and salinity structure of shelf water, we examine these properties on the coastal Alabama shelf, a relatively understudied region of the U.S. coastal zone. This paper focuses on variability at the seasonal and weather band time scales with the goal of developing a better understanding of the seasonal structure of the water column

* Corresponding author at: Department of Marine Sciences, University of South Alabama, Dauphin Island Sea Lab, 101 Bienville Blvd., Dauphin Island, AL 36528, USA. Tel.: +1 251 861 2141x7563; fax: +1 251 861 7540.
E-mail address: kpark@disl.org (K. Park).
[1] Present address: Korea Polar Research Institute, KORDI, Songdo Technopark, Incheon 406-840, South Korea.

0278-4343/$ - see front matter © 2011 Elsevier Ltd. All rights reserved.
doi:10.1016/j.csr.2011.03.001

offshore of a large freshwater source as well as quantifying the forcing relationships driving the observed structure. This work represents an extension of the hydrographic work conducted in the Mobile Bay area focusing on the impact of estuarine–shelf exchange on the shelf, and compliments one recent shelf circulation study based on, but using different aspects of, the same regional data set (Dzwonkowski and Park, 2010). In the following section, the study area is described as well as previous research around the region. Section 3 describes the data and analysis methods used in this study. The results and discussion are provided in Section 4 and conclusions in Section 5.

2. Regional background

The Alabama shelf is in the central region of the northern Gulf of Mexico (Fig. 1). A key geographic feature of the region is Mobile Bay, a shallow drowned river-valley estuary. The bay receives the second largest river discharge into the Gulf of Mexico after the Mississippi–Atchafalaya River system, primarily from the Alabama and Tombigbee rivers with a resulting drainage basin of 115,467 km^2 (http://www.mobilebaykeeper.org/about-us/mobile-bay-watershed). While the bay itself is relatively large, approximately 50 km in length (north–south) and 14–34 km in width (east–west), its connections to the Gulf and Mississippi Sound are narrow and shallow (Schroeder and Wiseman, 1986). Thus, the large amounts of freshwater, with long-term (1976–2009) mean daily discharge of 1715 m^3 s^{-1}, are confined to two relatively narrow passes with the Main Pass, the bay's direct connection to the Gulf, controlling an estimated 85% of the exchange (Schroeder, 1979). There is significant seasonality in the river discharge with maxima occurring in late winter/early spring and minima occurring in late summer/early autumn (Stumpf et al., 1993). The climatology of local winds (Huh et al., 1984; Schroeder and Wiseman, 1985) shows the late fall and winter winds coming from the northern quadrant with intermittent episodes of strong southwest and northwest winds. The spring winds shift to the southeast, further weakening and shifting to the southern quadrant during the summer.

While estuarine outflow plumes have been regularly observed (Dinnel et al., 1990), the structure and extent of the plumes on the shelf have received only cursory examination (Abston et al., 1987; Dinnel et al., 1990; Stumpf et al., 1993). In terms of basic hydrographic information in the shallow coastal waters on the Mississippi–Alabama shelf, there have only been a few studies, all of which were limited in their spatial and temporal coverage. Turner et al. (1987), summarizing the findings of the previous studies, reports observation of both thermal and haline stratification with the strongest pycnocline developing between 5 and 10 m and temperature and salinity differences of 10 °C and 20 psu, respectively. Jochens et al. (2002) reports spatially synoptic maps of the hydrographic conditions in the northeast Gulf of Mexico, showing large spatial and temporal variability on the Mississippi–Alabama shelf.

Several regional circulation studies examine the temperature/salinity structure in the northern Gulf of Mexico (He and Weisberg, 2002, 2003; Weisberg and He, 2003; Morey et al., 2003a, 2003b, 2005, 2009). However, none of these efforts focus on the near-shore region (shallower than 30 m isobath) of the Alabama shelf. The results of these circulation studies as well as other observational hydrographic studies throughout the northern Gulf of Mexico (Huh et al., 1984; Cochrane and Kelly, 1986; Dinnel and Wiseman, 1986; Wiseman and Kelly, 1994; Wiseman et al., 1997; Weisberg et al., 2000; Virmani and Weisberg, 2003) show that seasonal summer stratification and winter mixing dominate the water column structure but synoptic scale variability in oceanic processes is a critical factor in controlling temperature/salinity variability on the shelf. While many hydrographic studies have been conducted on the shelf in the eastern and western Gulf of Mexico, relatively few have focused on the shelf region directly impacted by Mobile Bay.

3. Materials and methods

3.1. Data source

A mooring station (CP in Fig. 1) with a mean depth of 20 m, about 20 km offshore of Dauphin Island, Alabama, has been maintained since November 2004 by the Fisheries Oceanography in Coastal Alabama (FOCAL) group of the Dauphin Island Sea Lab. The station has a mooring line instrumented with two SeaBird

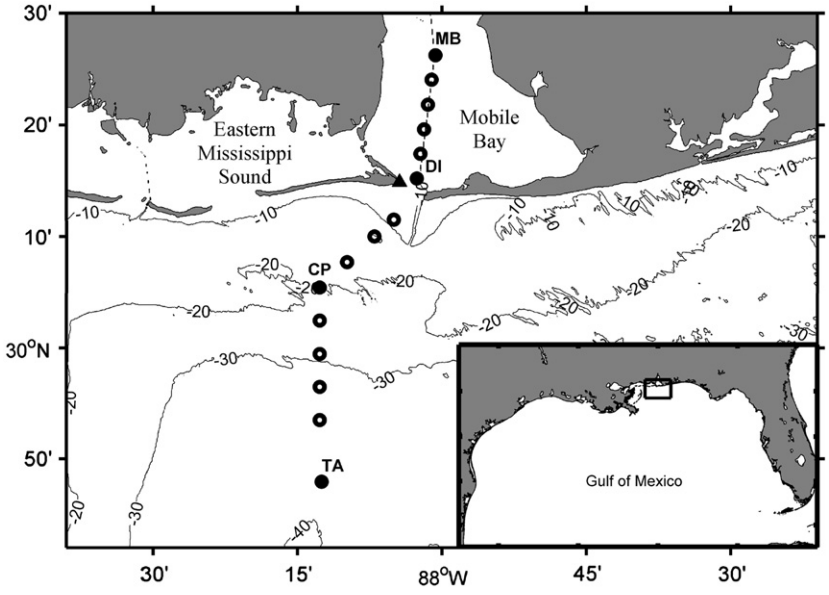

Fig. 1. Map of the Alabama shelf and lower Mobile Bay, showing the bathymetry (m), the stations for the CTD surveys (circles), mooring station (CP), and the NOAA National Data Buoy Center station DPIA1 on Dauphin Island (▲). The filled circles indicate the stations labeled in the across-shelf transects in Fig. 6.

MicroCats (SBE 37-SMP) at the surface (4.3 m) and bottom (20 m) and 10 SeaBird thermistors (SBE 39) at $\Delta z = 1$–1.5 m intervals. The data at a depth of 4.3 m are referred to as the surface data because the CTD casting data show that this depth is typically in the surface mixed layer (Section 4.1.3), except in the presence of estuarine outflow plumes which can result in vertical gradients shallower than a depth of 4.3 m (Section 4.3.2). All instruments were programmed to record 20 min averages. The resulting data set includes time series of salinity and density at surface and bottom and time series of vertical profiles of temperature. The instruments were regularly serviced, but intermittent gaps in the data due to bio-fouling or other instrument malfunctions did arise, particularly in the salinity data. The handling of these gaps is discussed in Section 3.2 (Data Analysis).

Another component of the FOCAL program is ship-based surveys with castings of SeaBird Sealogger CTD (SBE 25) at 15 stations along a 75 km transect starting from the Middle Bay Lighthouse in Mobile Bay and extending out to the 35 m isobaths on the shelf (MB to TA in Fig. 1). The upstream six stations are within Mobile Bay, and, except station MB, are located in the 12–14 m deep ship channel. The CTD surveys started in 2007, and the data used in this study were collected on May 16, July 11, August 1, August 30 and December 12, 2007; February 19, July 28, August 27 and November 20, 2008; and May 05, June 26 and July 16, 2009. The CTD casting data for temperature, salinity and density from these 12 surveys were interpolated to a 0.5 m (vertical) by 1 km (across-shelf) plane along the transect.

For forcing functions, air temperature and wind data were collected from the NOAA National Data Buoy Center station DPIA1 at Dauphin Island (Fig. 1). In general, the data are continuous over the study period with all gaps less than 6 h (Figs. 2a, b). For analysis techniques that require a gap free data set, these gaps were filled using linear interpolation. The (u, v) components of the wind data are well orientated with the along- and across-shelf directions, respectively. From these winds, the surface wind stress was estimated following Large and Pond (1981). The data for daily river discharge were collected from the USGS gaging stations at Claiborne L&D in Alabama River and at Coffeeville L&D in Tombigbee River. Their sum (Fig. 2c) was used as a total freshwater discharge into Mobile Bay, following Park et al. (2007).

3.2. Data analysis

To quantitatively examine the observed variability and the possible forcing mechanisms, several processing steps and analysis techniques are performed on the data. Given the notable gaps in the data, the time series are separated into three quasi-continuous segments (Fig. 2d): segment 1 from October 2004 until February 2006, segment 2 from May 2006 until June 2007, and segment 3 from August 2007 until March 2008. The data are hourly averaged to reduce high frequency signals not important for the oceanic processes of interest in this study. Short gaps (≤ 4 h) in the hourly data are filled using linear interpolation, an adequate processing because the highest frequency (tidal and near-inertial) processes operate on $\sim$24 h cycles in the study region (30°N). This processing, however, does not eliminate all the data gaps. The analysis techniques sensitive to data gaps are conducted with sections of the time series with no gaps. In cases where the resulting time series are significantly shortened, either the analysis is not conducted or the size of the reduced time series is specifically noted. A brief description of the analysis techniques employed in this study, including least squares fit, spectral analysis, filtering, and correlation analysis, is given below, and the details pertinent to these techniques are individually noted in Section 4 (Results and Discussion) as they are used in specific ways as dictated by the character of the data.

With the annual signal being the longest time scale apparent in the data, its contribution to the variance is quantified using a least squared fit approach, in which a harmonic function of the form

$$y = A\sin\left(\frac{2\pi}{T}t\right) + B\cos\left(\frac{2\pi}{T}t\right) + C \quad (1)$$

is fitted to each of the three segments; y is the time series, T is the period (365.25 d), and t is time in d. The constants A, B, and C are harmonic coefficients, where C is the series mean, $(A^2+B^2)^{1/2}$ is the annual amplitude, and $\tan^{-1}(B/A)$ is the phase relative to the center time of the data which has been adjusted to January 1 to facilitate comparison. Given the shorter (<1 yr) duration of segment 3 and its similar general behavior compared to other segments, only the results from segments 1 and 2 are presented.

Seasonal differences are most clearly identifiable in the temperature data (Fig. 2d). The time series are further separated into summer (May–August) and winter (November–February) periods, allowing for a two month transitional buffer between seasons. The summer months are selected to include the period of rising temperature with thermal stratification, whereas the winter months are selected to include the period of falling temperature with thermal inversion. This seasonal separation into summer and winter also coincides with the periods following the annual maxima and minima in river discharge, respectively (Fig. 2c). The separation gives three winter (W1, W2, and W3) and two summer (S1 and S2) time series with a near complete data record in each series. Likewise, the CTD casting data are also grouped and averaged into winter (3 surveys) and summer (9 surveys) periods to generate seasonal mean pictures of the horizontal and vertical structure of the water column in lower Mobile Bay and on the shelf. The small number of surveys used in averaging, particularly for winter ($n=3$), may result in a constrained representation of the water column structure. Yet, consistency between the CTD data and the time series at station CP suggests a representativeness of the CTD-based seasonal mean transects at the mooring site and presumably for the entire transect: see Section 4.1.3 (Seasonal Variation).

To examine the higher frequency variability over months to days, anomaly time series, defined as the hourly data minus the annual signal, are subjected to standard spectra analysis using the pwelch method (see the MATLAB 8.0 Users' Guide). Guided by the results of the spectral analysis and the time scales of the forcing functions, we further analyze the data through three temporal perspectives: sub-tidal (>1.7 d), synoptic (1.7–15 d), and low frequency (>15 d). The sub-tidal signal, obtained by low-pass filtering (40 h) the data using a Lanzcos filter, contains all variability resulting from processes operating at time scales greater than tidal and near-inertial periods in this region. The synoptic signal is obtained by band-pass filtering (1.7–15 d) the data using a Lanzcos filter to capture variability at the higher sub-tidal frequencies of the weather band (2–10 d) and near-weather band (<15 d). The low frequency signal, with the intention of examining longer time scales ranging from weeks to seasons, is obtained by daily averaging the data to make it compatible with the daily discharge data, which is then low-pass filtered (15 d) with a Lanzcos filter.

Time-lagged correlations are performed using these filtered signals to identify relationships between the water column layers and between the water column and the available forcing functions (air temperature, wind stress, and river discharge). Statistical significance is evaluated at the 95% confidence level using effective degrees of freedom given by the time series length and integral time scale of the data (T_D) calculated following Münchow and Chant (2000) as

$$T_D = \int C_{xx}(t)C_{yy}(t)\,dt \quad (2)$$

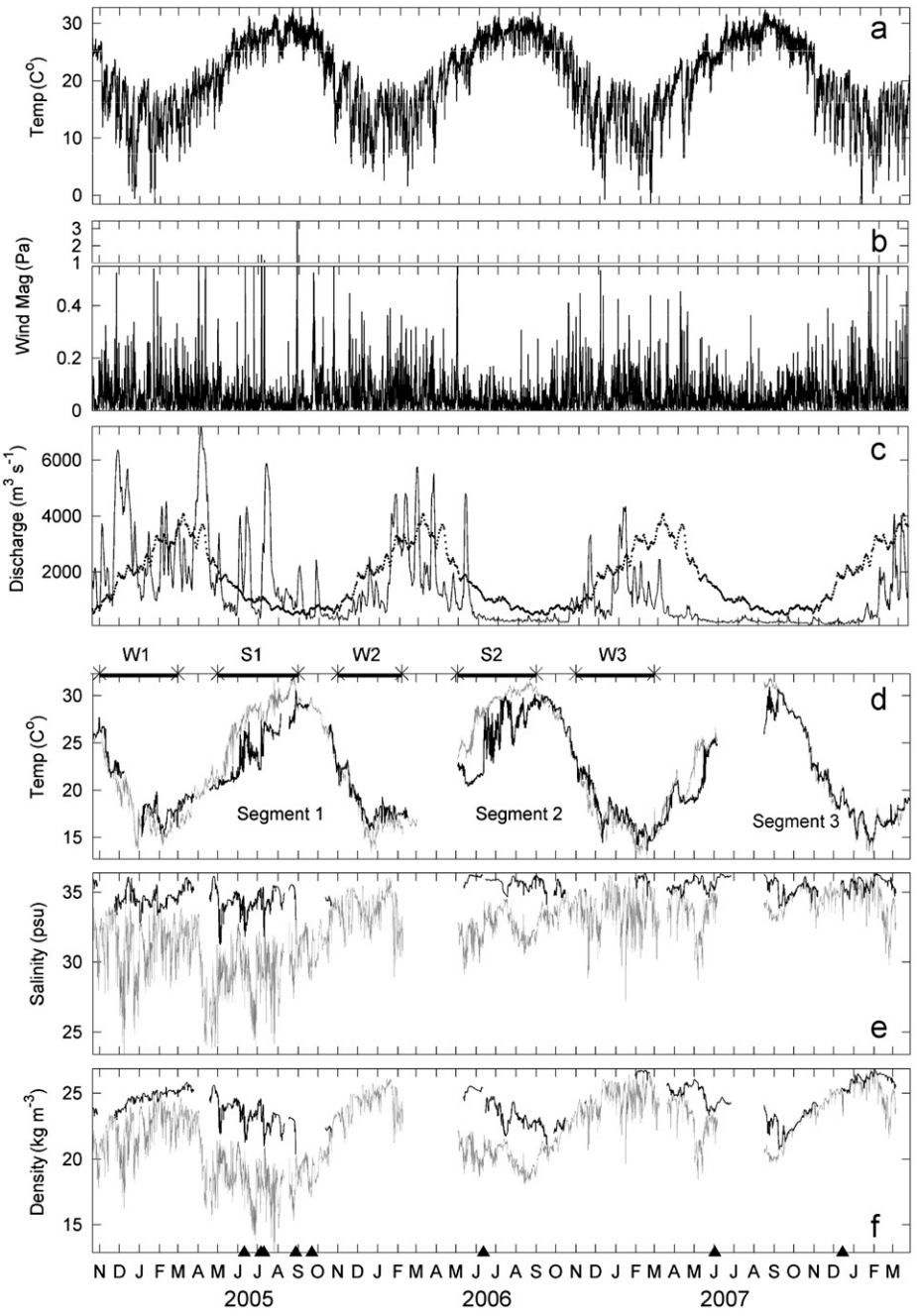

Fig. 2. Forcing functions including (a) hourly air temperature, (b) hourly wind stress magnitude, and (c) daily river discharge (solid line) with the long-term (1976–2009) mean discharge (dashed line), and hourly time series at surface (4.3 m: gray line) and bottom (20 m: black line) of station CP for (d) water temperature, (e) salinity, and (f) density. Note three segments, and three winter and two summer periods indicated at the top of (d). Tropical storms (▲) that affected the study region are indicated at the bottom of (f): Arlene (June 11, 2005), Cindy (July 6, 2005), Dennis (July 10, 2005), Katrina (August 28, 2005), Rita (September 22, 2005), Alberto (June 12, 2006), Barry (June 2, 2007), and Olga (December 15, 2007).

where C_{xx} and C_{yy} are the autocorrelation functions. For practical purposes, the integration time takes on a finite value of ± 30 or ± 120 d depending on the time scales of the processes analyzed. A more conservative estimate of 2 d is used when the resulting T_D is less than 2 d.

It should be noted that several analyses performed in this study are limited by small sample sizes, such as the segment analysis ($n=2$) and the seasonal analysis ($n=2$ or 3 for summer and winter, respectively). These small sample sizes limit this study's ability to make statistically significant statements about interannual variability. Consequently, the observed patterns in cases with small sample sizes should be considered qualitative, as necessitated by data limitation.

4. Results and discussion

4.1. Variations at different time scales

4.1.1. Overview

The data for temperature, salinity and density at surface and bottom of the mooring station show variability at a range of time scales. Qualitative descriptions of patterns and characteristics evident in the hourly data are given in this section, which is followed by quantitative examination of variability at various time scales in Sections 4.1.2–4.1.4. The long-term (1976–2009) mean river discharge in Fig. 2c provides a historical perspective

for the time-series segments and seasons shown in Fig. 2d. Segment 1 experienced average to above average discharge levels (wet) whereas segments 2 and 3 experienced very low discharge levels (dry). The segments' individual seasons generally reflect these conditions with W1 and S1 being wet and W2, S2, and W3 being dry.

The temperature data (Fig. 2d) are dominated by an annual cycle in both the surface and bottom depths, typical of a mid-latitude region, with the temperature peaking (or bottoming) during times slightly lagging the expected maximum (or minimum) of the solar insolation. The seasonal structure shows the summer months have the greatest thermal stratification. On the other hand, the winter months experience much more uniform temperatures in the vertical, often times with the bottom temperature warmer than the surface temperature.

The salinity data (Fig. 2e) are quite different from the temperature data. Most apparent is the difference in the character of the annual signal. In the surface salinity, not only is the annual signal weak, particularly in 2006–2007, but there is notable year to year variability. The limited bottom salinity data show no discernable annual signal with the variability oscillating around nearly constant values for all three segments. In terms of seasonal patterns, the notable winter–summer differences in temperature are much less clear in salinity.

The density structure (Fig. 2f) is affected by both temperature and salinity. There is a strong annual signal in both the surface and bottom densities corresponding with that of the temperature. There are also notable high frequency modulations, particularly in surface density, the largest of which clearly corresponds with salinity fluctuations. While the water column appears to be stable, i.e. bottom water denser than surface water, most of the study period, the surface and bottom density differences are quite variable, with a general trend for stronger density stratification in the summer months.

It is clear that vertical differences in temperature, salinity, and density are very sensitive to episodic events and that the characteristics of the winter and summer events are different. During the summer, there are mixing events with the sharp and oppositely directed changes in surface and bottom densities (e.g. tropical storms, ▲, in Fig. 2f). Note that not all mixing events are associated with tropical storms (e.g. May 5, 2005 and July 14, 2006). During the winter, on the other hand, there are stratifying events with sharp drops in the surface density associated with large river discharge levels, but with little to no corresponding change in the bottom density (e.g. November 15, 2004, December 2, 2004, and February 3, 2008).

4.1.2. Annual signal

The observed differences in the annual signals are quantified using annual harmonic fits of the hourly data (Eq. (1)) and the results are summarized in Fig. 3. As expected, the temperature has the strongest annual signal accounting for 95% of the variance at the surface and 83–88% at depths. The amplitudes range from 8.1 to 4.5 °C deceasing with depth, and the phases also change with depth having a surface–bottom difference of 18–19°, i.e. the bottom temperature lagging the surface temperature by 18–19 d in its annual cycle. There is little year to year variability in the annual temperature signal during the study period, i.e. similar variance explained, amplitude, and phase between segments 1 and 2. However, the annual signal in the salinity data is quite

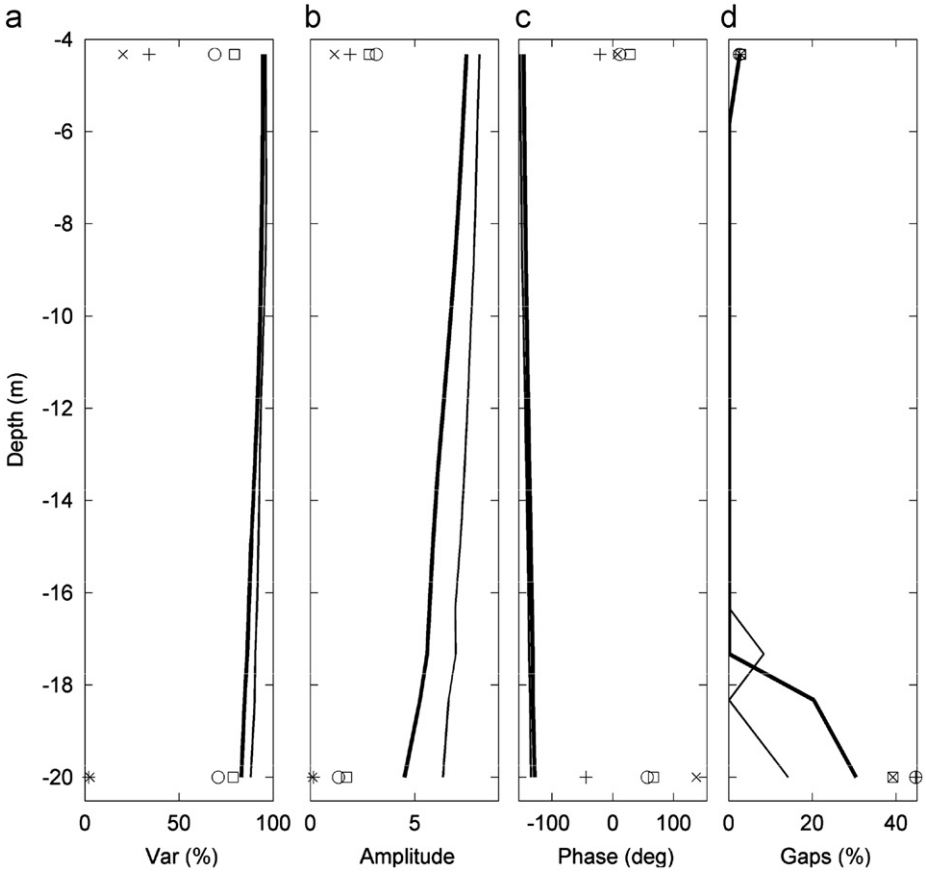

Fig. 3. Summary of the annual signal from the least squares fits for (a) percent variance, (b) amplitude, (c) phase relative to January 1, and (d) percent data gap. The lines represent the temperature profiles for segments 1 (thick line) and 2 (thin line). The symbols indicate salinity (+ and × for segments 1 and 2, respectively) and density (○ and □ for segments 1 and 2, respectively).

different. The annual surface salinity signal explains much less variance and has notable year to year differences, 34% in segment 1 compared to 14% in segment 2, indicating a much weaker annual signal and stronger year to year differences compared to the temperature. The high percentage of data gaps in the bottom salinity for both segments will not allow us to examine the annual signal. The density data represent a mixture of the temperature and salinity data. There is a clear annual signal, but it accounts for a smaller variance compared to the temperature. There also is some year to year variability in the annual density signal, accounting for 70% of the variance in segment 1 compared to 79% in segment 2. The phases of the annual signals are relatively consistent with our expectation, with the temperature minima occurring in the winter and the surface salinity minima occurring in the summer.

4.1.3. Seasonal variation

4.1.3.1. Mooring site. As a first-order examination of the winter and summer seasons, the time averaged vertical structures of the water column at the mooring site are shown for three winter and two summer periods in Fig. 4. In all three winter periods, temperature increases smoothly from the surface to the bottom. The surface to bottom difference, however, is very small and so are the interval temperature differences ($<0.2\ ^{\circ}C$) between the thermistor depths ($\Delta z=1$–1.5 m), indicative of a well mixed water column. Garvine (2004) uses this temperature difference as a criterion for a boundary layer threshold. Yet, the presence of a mean temperature inversion suggests that some level of salinity stratification is necessary for water column stability, which is supported by the salinity data with the surface water fresher than the bottom water. Year to year variability is apparent in the winter. W1 has a warmer and fresher water column than W3, and also has larger surface–bottom differences in the temperature and salinity. During the summer, the temperature structure reverses. The vertical temperature gradients increase with a surface–bottom temperature difference of about $4\ ^{\circ}C$ and have larger depth interval differences, indicative of a stratified water column. The summer salinity is similar to the winter salinity, exhibiting notable year to year variability in both the surface and bottom means and in the surface–bottom differences, 5 psu in S1 compared to 2 psu in S2.

The seasonal variation in the vertical structure is further characterized by examining the depth-dependent nature of the fluctuations in the water column. The correlations relative to the surface of the sub-tidal temperature anomaly at each depth show contrasting structure between seasons (Fig. 5). During the winter, temperature fluctuations are coherent throughout the water column having significant correlations with *r*-values that generally decrease with depth. In contrast, the summer water column temperature variability becomes insignificantly correlated at shallow depths (7–12 m for S1 and S2), below which the temperature fluctuations are unrelated to the surface. The time series at depths that have insignificant correlations or have more than 10% data gaps show a wide range of *r*-values and lags that are unlikely to have physical meanings. This indicates a two-layered structure where the surface and bottom layers act as independent slabs, in sharp contrast to the relatively smooth structure of the winter periods in which temperature variations work their way down into the water column.

4.1.3.2. Across-shelf transect. Fig. 6 shows the seasonal mean transects based on the CTD data. We acknowledge the limited

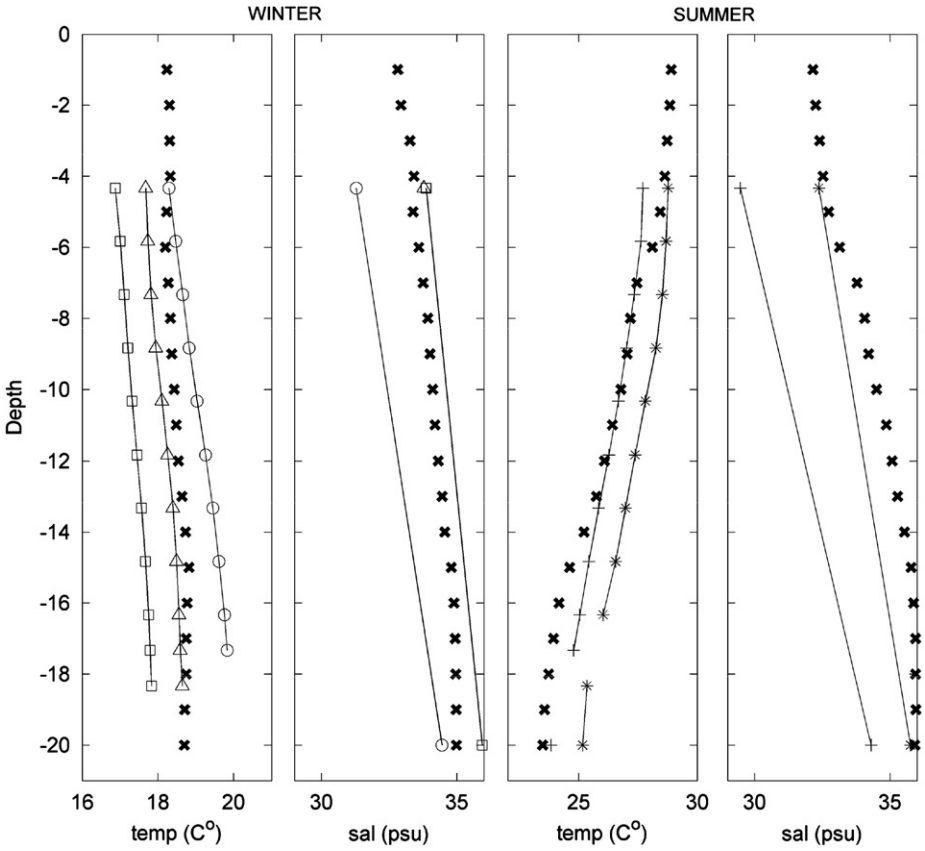

Fig. 4. Seasonal mean temperature and salinity for three winter (○, △, and □ for W1, W2, and W3, respectively) and two summer (+ and ∗ for *S*1 and *S*2, respectively) periods, and the corresponding profiles from the CTD casting data (×). The temperature data with $>10\%$ data gaps and the salinity data with $>20\%$ data gaps are not shown. Note that only surface salinity is available for W2.

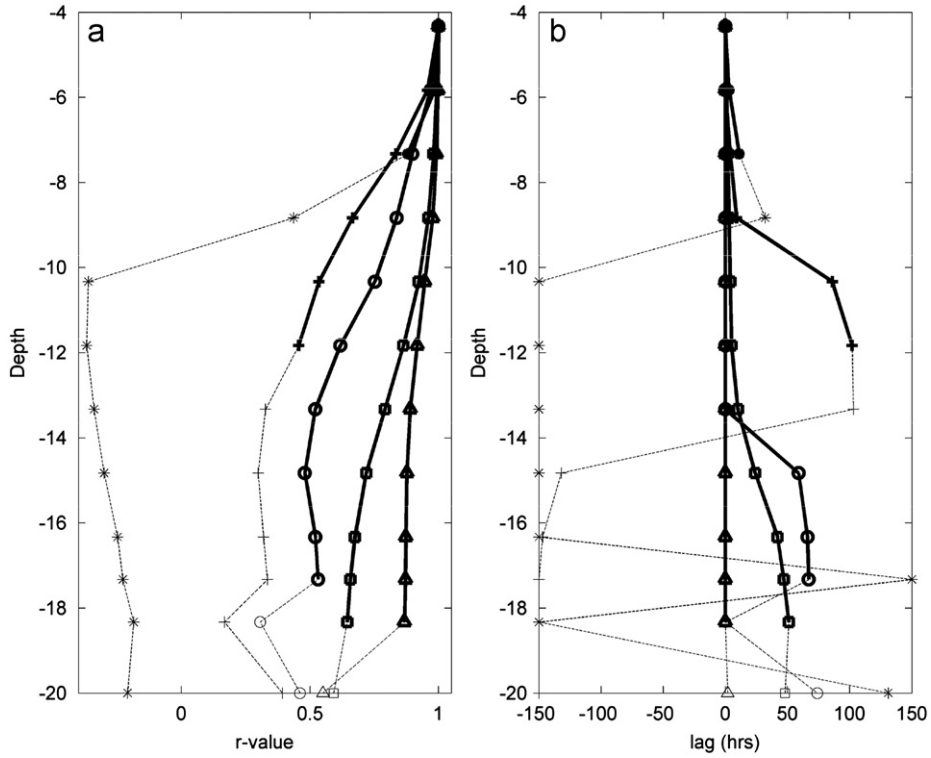

Fig. 5. Correlations relative to the surface of the sub-tidal (40 h low-pass filtered) temperature anomaly at each depth for three winter (○, △, and □ for W1, W2, and W3, respectively) and two summer (+ and ∗ for S1 and S2, respectively) periods: (a) maximum correlation coefficients and (b) their associated time lags. The data with > 10% data gaps or those with correlation coefficients not significant at the 95% confidence level are shown with thin dashed lines. Maximum lag allowed is 150 h.

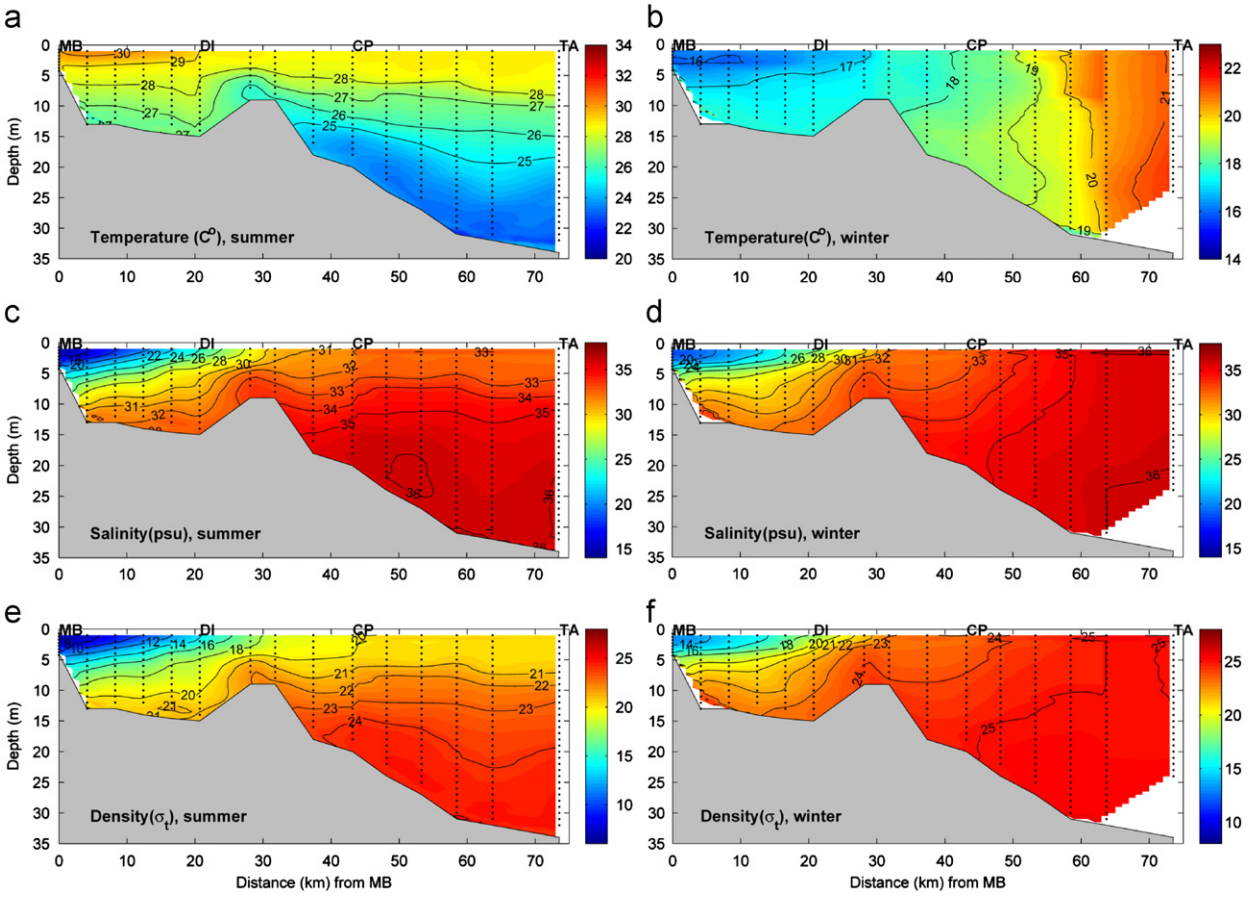

Fig. 6. Seasonal mean across-shelf transects during summer (May–August) and winter (November–February) based on the CTD data. Note the contour lines shift 2 units per contour in lower Mobile Bay to one unit per contour on the shelf. The black dots indicate locations of CTD cast data.

number of CTD surveys for winter (3 surveys) and summer (9 surveys) periods, and that all CTD surveys were conducted during low to normal discharge conditions. Yet, consistency between the CTD-based vertical profiles with those from the time series at station CP, particularly for those with low river discharge (W2 and S2 in Fig. 4), indicates that the transects in Fig. 6 may be representative of dry/normal conditions.

The across-shelf transect well illustrates the transition from estuary to shelf with distinctive seasonal variability (Fig. 6). In the estuarine section from stations MB to DI, there are strong vertical gradients in temperature and salinity, and thus density, in both the summer and winter. Progressing onto the shelf, stations DI to CP represent a transition zone in which vertical salinity stratification exists in both the summer and winter, albeit weak in the winter, but vertical temperature stratification exists only in the summer. In both the estuarine and transition zone inside of station CP, a temperature inversion exists in the winter but the density structure remains stable owing to salinity stratification, consistent with the time series at station CP (Fig. 4). The shelf zone offshore of station CP is associated with strong vertical gradients in temperature and salinity, and thus density, in the summer, whereas the gradients are mostly horizontal in the winter. These seasonal variations in gradients are consistent with the sea surface temperature maps for the west Florida shelf (Liu et al., 2006: Fig. 5) and modeled salinity transect on the Mississippi–Alabama shelf (Morey et al., 2003a: Fig. 6). The shift from the transition zone to the shelf is marked by a weak frontal zone around station CP whose expression changes with season. During summer, the shelf isohalines, and isopycnals, are relatively horizontal offshore of station CP at which their orientation steepens forming a front that extends down to mid-depth. The winter front is less distinct, with little influence of the Mobile Bay plume offshore of station CP.

4.1.4. Months-to-days time scales

The power spectra of the temperature and salinity anomalies in general are similar for all segments (not shown). The spectra are primarily red, with the high frequency signals of periods < 40 h accounting for 4–12% and 12–15% in the temperature at all available depths and the surface salinity, respectively. The high frequency bands are dominated by a diurnal peak associated with tidal and near-inertial motion. The low frequency energy begins increasing around 0.5 cpd (2 d) and generally increases over the lower frequencies indicating that the weather band (2–10 d) and weekly to monthly signals are important in controlling temperature and salinity variability. While the variability in this frequency band can be relatively small when compared to the annual signal, particularly in temperature (e.g. temperature anomaly standard deviation $=1.0$–$1.5\ ^{\circ}$C), these fluctuations have important affects on the water column structure. As mentioned earlier, several of these short term fluctuations, mostly associated with tropical storms, bring about complete thermal mixing and nearly complete salinity mixing, resulting in weak, if any, stratification (Figs. 2d–f).

4.2. Relationships with forcing functions

We examine the relationships between the temperature/salinity variability and available forcing parameters including air temperature, river discharge, and wind stress. Air temperature varies at a wide range of time scales, with its annual signal used as a proxy for the solar heating cycle and its higher frequency fluctuations being related to weather band processes. River discharge exhibits strong seasonality and is primarily energetic at low frequencies (> 15 d). Wind stress is expected to impact variability through mixing and advective processes. In terms of advective processes, this study focuses on the impacts of the direct estuarine response to the across-shelf (north–south) wind along the axis of Mobile Bay and the shelf response through Ekman dynamics to the along-shelf (east–west) wind. The estuarine and shelf responses have been shown to operate at weather band time scales of 2–4 and 3–20 d, respectively, in driving the shelf–estuarine exchanges for Mobile Bay (Schroeder and Wiseman, 1986; Wiseman et al., 1988).

4.2.1. Correlations between forcing functions

Since the forcing functions are not always independent, their correlations are examined to guide analysis and interpretation of the results in the relationship between the observed variability and forcing parameters. The cross-correlations between the forcing functions are examined at both the low frequency and synoptic time scales as these are the time scales in which the forcing–response relationships are examined. Table 1 shows the correlations between the low frequency signals (> 15 d) of the forcing functions for segments 1 and 2. Most of the correlations are not statistically significant, however, there is a significant and consistent, i.e. similar r-values and lags in both segments, relationship between air temperature and the across-shelf wind stress. The positive correlations indicate that decreased (or increased) air temperature anomaly is associated with negative offshore (or positive onshore) wind. This is consistent with the behavior of the seasonal/monthly wind patterns that offshore north (or onshore south) winds are associated with colder (or warmer) air temperature.

Table 2 shows the correlations between the forcing functions at the synoptic time scales (1.7–15 d), conducted over individual seasons. The along- and across-shelf wind stresses have strong negative correlations for all seasons, with somewhat higher r-values for the summer periods. It indicates that the wind components often vary together but in opposite directions, i.e. north (or south) wind associated with west (or east) wind, consistent with previous observations (Huh et al., 1984; Schroeder and Wiseman, 1985). In addition, there are significant correlations between both the across- and along-shelf wind stress and air temperature during the winter periods. Statistically, these results may indicate that any one of the three correlations could be attributed to the other two. Physically, however, the positive correlations between the across-shelf wind stress and air temperature are consistent with previous observations of cold air outbreaks in the study region, i.e. warm air advected by south winds prior to the front arrival and cold air advected by north winds during and post-front (Huh et al., 1984). The negative associations between the along-shelf wind stress and air temperature, therefore, are likely the result of a positive correlation between the across-shelf wind stress and air temperature and a negative correlation between the along- and across-shelf wind stresses.

Table 1
Correlations between forcing functions at the low frequency time scales (> 15 d).

Parameter[a]	Segment 1		Segment 2	
	r-Value[b]	Lag[c]	r-Value	Lag
$\tau_{w,al}$ vs. $\tau_{w,ac}$	−0.36	1	(−0.27)	18
T_{air} vs. $\tau_{w,al}$	(−0.22)	0	−0.42	0
T_{air} vs. $\tau_{w,ac}$	0.58	2	0.60	2
Q_f vs. $\tau_{w,al}$	(0.14)	22	(−0.27)	12
Q_f vs. $\tau_{w,ac}$	(0.22)	8	(−0.43)	25

[a] Along-shelf wind stress ($\tau_{w,al}$), across-shelf wind stress ($\tau_{w,ac}$), air temperature (T_{air}), and river discharge (Q_f).
[b] Values in parentheses are not significant at the 95% confidence level.
[c] Values represent days in which the first parameter follows the second.

Table 2
Correlations between forcing functions at the synoptic time scales (1.7–15 d).

Season[a]	W1		W2		W3		S1		S2	
Parameter[b]	*r*-Value[c]	Lag[d]	*r*-Value	Lag	*r*-Value	Lag	*r*-Value	Lag	*r*-Value	Lag
$\tau_{w,al}$ vs. $\tau_{w,ac}$	−0.67	−9	−0.64	−8	−0.73	−13	−0.87	−6	−0.76	0
T_{air} vs. $\tau_{w,ac}$	0.76	8	0.77	9	0.73	8	(−0.14)	7	(0.25)	0
T_{air} vs. $\tau_{w,al}$	−0.41	16	−0.57	19	−0.55	19	(0.13)	19	(−0.12)	−55

[a] See Fig. 2d.
[b] Along-shelf wind stress ($\tau_{w,al}$), across-shelf wind stress ($\tau_{w,ac}$), and air temperature (T_{air}).
[c] Values in parentheses are not significant at the 95% confidence level.
[d] Positive (or negative) values represent hours in which the first parameter follows (or leads) the second.

Table 3
Correlations between the surface and bottom mass properties (temperature and salinity) and forcing functions at the synoptic time scales (1.7–15 d).

Season[a]	W1			W2			W3			S1			S2		
Parameter[b]	*r*-Value[c]	Lag[d]	θ[e]	*r*-Value	Lag	θ	*r*-Value	Lag	θ	*r*-Value	Lag	θ	*r*-Value	lag	θ
Air temperature															
T_S vs. T_{air}	0.50	23		0.39	21		0.54	17		0.36	12		0.42	26	
T_B vs. T_{air}	(-0.11^{II})	7		(0.15^{I})	9		0.36^{I}	68		(-0.25^{II})	2		(0.27)	101	
Wind stress															
T_S vs. τ_w	0.34	24	310	0.40	36	345	0.49	28	290	0.29	54	70	(0.20)	80	350
S_S vs. τ_w	0.45	8	10	0.38	18	320	0.63	5	350	(0.26)	96	195	0.33	0	55
T_B vs. τ_w	0.35^{II}	52	80	0.40^{I}	37	60	0.29^{I}	0	130	(0.19^{II})	10	245	0.57	40	240
S_B vs. τ_w	0.37	40	60	–	–	–	–	–	–	0.45	30	60	(0.33)	105	65

[a] See Fig. 2d.
[b] Air temperature (T_{air}), wind stress (τ_w), water temperature at surface (T_S) and bottom (T_B), and salinity at surface (S_S) and bottom (S_B).
[c] Values in parentheses are not significant at the 95% confidence level. Values with the superscripts I or II indicate that the correlation was calculated with the data one or two instruments, respectively, below (or above) the upper- (or lower-) most instrument for surface (or bottom).
[d] Positive values represent hours in which the first parameter follows the second.
[e] Angle (θ) is wind direction that gives maximum positive correlation; θ=0° for south wind and increases in clockwise direction.

4.2.2. Long period time scales

The annual signal in the temperature is presumed to be caused by the annual cycle in solar heating, which generally remains constant over the 3 yr of the study period (Fig. 2a). As such, the annual signal amplitudes at the surface are very similar between segments 1 (7.5 °C) and 2 (8.1 °C) (Fig. 3b). The reduced amplitude from the surface to the bottom (7.5–4.5 °C and 8.1–6.3 °C for segments 1 and 2, respectively, in Fig. 3b) and the phase lag at the bottom (18 and 19 d for segments 1 and 2, respectively, in Fig. 3c) indicate decreased and delayed heat flux at depths during the annual solar heating cycle. This phase lag in the bottom temperature may help the formation of the summer stratification and winter inversion (Fig. 4). However, the spatial structure of the seasonal mean temperature and salinity transects (Fig. 6) suggests that the surface–bottom differences may also be related to estuarine–shelf exchange: see Section 4.3 (Estuarine Influence on the Shelf).

Given the relatively weak annual signal in the salinity, the low frequency signals (>15 d) of the salinity and river discharge are compared using time-lagged correlation. Due to the larger decorrelation time-scales of low frequency processes, correlation analysis is conducted over segments rather than individual seasons. As such, any gaps remaining from the initial conservative gap filling applied to the hourly data are further filled using linear interpolation. In the surface salinity, only a limited portion of the low frequency data contains gaps ($<3\%$ in each segment) and the individual gaps are relatively short ($<\frac{1}{3}$ of the decorrelation time scale), so the overall effect on the correlation analysis is expected to be minimal. However, there are considerable gaps in the bottom salinity and the resulting relatively shorter signal lengths make it difficult to obtain statistically significant results (not shown). A significant correlation exists between the surface salinity and discharge for segment 1 ($r=-0.58$ with a lag of 11 d). The negative correlation is consistent with the physical expectation of increased discharge decreasing shelf salinity and the lag of 11 d is in line with previous estimates, 5–9 d (Schroeder, 1979) to 9 d (Wiseman et al., 1988), for discharge at the gauging stations reaching the bay mouth, about 20 km upstream of the mooring site. No significant correlation is found over segment 2 because unusually low discharge during this period leaves little signal on the surface salinity: see Section 4.3 (Estuarine Influence on the Shelf). Note, however, there are occasional episodes of large river discharge that are associated with declines in the surface salinity (e.g. May 5, 2006, November 20, 2006, and January 6, 2007), showing the dependency of surface salinity on discharge at the mooring site.

4.2.3. Synoptic time scales

The correlations at the synoptic time scales (1.7–15 d) are shown for the winter and summer periods in Table 3. The water and air temperatures are correlated at the surface with time lags of 12–26 d for all five periods but are uncorrelated at the bottom in all but one period, W3. These correlations demonstrate that the weather band variability in air temperature impacts the surface layer but not the lower layer of the water column. While the surface correlations during the winter periods appear to have higher correlations, these results are likely inflated because of positive correlations between surface temperature and the across-shelf wind stress, a driver of direct estuarine response, during the winter periods as discussed below.

Strong negative correlations between the along- and across-shelf wind stresses (Table 2) complicate the analysis of the temperature/salinity response to wind stress as a component correlation could result from its relationship with the other component rather than an actual physical response. As such, the

correlations with the wind stress are determined by computing the maximum r-value and its associated time lag with a rotation of the wind angle at 5° intervals to minimize any potential biasing from the correlation between two wind components. The resulting correlations, despite relatively small r-values, do present evidence about mechanisms impacting the temperature/salinity variability.

During the winter periods, the surface properties are positively correlated with south wind (θ=290°–10° in Table 3). The positive correlations in the surface temperature can be attributable to the positive correlations between air temperature and the across-shelf wind stress (Table 2) and those between surface temperature and air temperature (Table 3). The positive correlations in the surface salinity, however, demonstrate the importance of an estuarine response to the across-shelf wind stress in the surface layer where negative north (or positive south) wind stress would be conducive to forcing fresher, colder estuarine (or saltier, warmer offshore) water onto the shelf. The bottom properties also are positively correlated with the wind stress, but the angles are typically in the eastern quadrant (θ=60°–130°), indicating an increased importance of the along-shelf wind component. This is consistent with Ekman coastal transport in bottom boundary layer, where positive west (or negative east) wind stress would cause offshore (or onshore) Ekman transport along the surface, which in turn would advect saltier, warmer shelf (or fresher, colder estuarine) water onshore (or offshore) along the bottom.

During the summer periods, the temperature/salinity correlations with the wind stress are not as consistent as the winter results (Table 3). It, however, is not unexpected given virtually no (very weak) across-shelf temperature (salinity) gradients around station CP (Figs. 6a, c). Two significant surface correlations, with smaller r-values compared to the winter periods, show a consistent shift in the wind angle (70° and 55°). In the bottom temperature data, the significant positive correlation with the east wind (240°), along with those correlations with the west wind during the winter periods, is consistent with the reversal of the seasonal across-shelf temperature gradients (Figs. 6a, b). As in the winter, the angles of best correlation remain in the eastern quadrant for the bottom salinity (60°). The shift in wind angles for the surface and relatively consistent wind angles for the bottom, then, result in both the surface and bottom properties correlated with the along-shelf wind component, suggesting an increased importance of coastal Ekman transport during the stratified summer season.

4.3. Estuarine influence on the shelf

The presence of Mobile Bay has a notable impact on the shelf hydrography and its physical forcing response at various time scales. It is mainly through river discharge at the low frequency time scales (>15 d) that Mobile Bay affects the magnitude and extent of the estuary's influence on the shelf. At the synoptic time scales (1.7–15 d), it is mainly through the estuarine response to the across-shelf wind for the surface properties whereas through the shelf Ekman response to the along-shelf wind for the bottom properties.

4.3.1. Influence at long period time scales

The large discharge differences result in much fresher shelf conditions with lower salinities of 31.3–34.5 psu in segment 1 (average of 2000 $m^3 s^{-1}$) compared to 33.3–35.7 psu in segment 2 (average of 780 $m^3 s^{-1}$) (Fig. 2). In addition, a significant correlation between salinity and discharge exists only for segment 1, but not for segment 2, likely the result of the much lower discharge for the latter; the long-term (1976–2009) mean discharge is 1715 $m^3 s^{-1}$ for comparison.

There are clear seasonal differences in the shelf salinity structure related to the exchange with Mobile Bay. The CTD-based seasonal mean transects (Fig. 6) show the influence of seasonal variability in river discharge on the shelf salinity distribution. During the summer the low-salinity water spreads offshore beyond station CP resulting in a strongly stratified water column over the shelf, whereas during the winter the low-salinity water is confined in the lower bay and the inner shelf inside of station CP resulting in a weakly stratified water column over the shelf, consistent with the model results in Morey et al. (2003a: Fig. 6). Thus, seasonal changes in the hydrographic gradients in Fig. 6 are directly linked to Mobile Bay and its exchange with the shelf. Note that the CTD data are from 12 surveys conducted during low to normal discharge conditions. Hence, salinity stratification would be stronger than that in Fig. 6 if based on data collected during average or above average discharge conditions.

The time series data provide evidence of interannual variability in the vertical salinity structure during a given season and its relationship to river discharge (Fig. 4). Of the five seasons, W1 (average discharge of 2770 $m^3 s^{-1}$) is the wettest and S1 (1770 $m^3 s^{-1}$) is the second wettest, both of which are well above the respective long-term seasonal mean discharges for the winter (2250 $m^3 s^{-1}$), and summer (1090 $m^3 s^{-1}$). As a result, these two periods have the freshest mean conditions as well as the largest surface–bottom salinity difference (Fig. 4). The remaining periods, W2, W3, and S2 with respective average discharges of 1510, 1420, and 560 $m^3 s^{-1}$, represent low discharge conditions, having higher salinities and smaller vertical salinity gradients.

4.3.2. Influence at synoptic time scales

At the synoptic time scales, the estuarine response to the across-shelf wind component, i.e. wind forcing along the estuary axis, becomes important in determining the estuarine–shelf exchange and thus affecting the shelf hydrography (Table 3). The tendency of the surface data at station CP to respond to estuarine forcing is likely a result of its location being in a region directly affected by the Mobile Bay plume. Dinnel et al. (1990) report satellite-derived mean plume characteristic of 28.5 km in length and 12 km in width with a mean angle of 193°, which effectively puts the average plume position over station CP. Furthermore, the fact that the observed estuarine response to the wind stress is surface limited is consistent with the shallow discharge of Mobile Bay (<5 m deep: Stumpf et al., 1993). The synoptic variability in the bottom properties, however, is associated more with the along-shelf wind component, consistent with the shelf Ekman response to the wind stress.

The presence of the Mobile Bay plume at the study site can lead to potential differences between the true surface conditions and the conditions at the shallowest depth of the mooring (4.3 m). Stumpf et al. (1993) report plumes as thin as 1 m, extending as far off as 30 km from shore. They also show that a very high density interface decouples the plume water from the water below, making only the thin plume water rapidly respond to the across-shelf wind. While this does not change any of the results of this study, it could modify the interpretation of the "surface" conditions during plume events at the mooring site. The CTD data at the CP mooring site show salinity variation in top 4 m of water column ranges from 0 to 1.7 psu (mean of 0.6 psu). Thus, the upper most mooring instrument at 4.3 m is representative of the surface layer except during very thin episodic plume events. Another point to note is that the along-shelf gradients in the mass properties may be important, particularly during plume events, but are not considered in this study. Then, the across-shelf

variability (e.g. Fig. 6) could have contributions from along-shelf advection, and may not solely be a consequence of interactions with Mobile Bay.

4.3.3. Wintertime temperature inversion

The wintertime temperature inversion is present at the synoptic time scales at the mooring site (Fig. 2d) as well as at the seasonal time scales (Fig. 6b) over the lower bay and the inner shelf inside of station CP. The mean winter CTD transect (Fig. 6d) shows relatively strong stratification inside of station CP, indicative of the influence of river discharge, which may allow the temperature inversion produced by surface cooling to persist. Further offshore with weak or no stratification the temperature inversion cannot be sustained as convection and/or wind mixing becomes more dominant. Additionally, bottom advection of warmer, saltier offshore water may also have played a role at the synoptic time scales as indicated by significant correlations between the wind stress and bottom temperature/salinity (Table 3). Thus, the shelf advection and estuarine–shelf exchange processes act to support the temperature inversion resulting from regional surface cooling over the lower bay and the inner shelf inside of station CP.

5. Conclusions

Time series of water column temperature and surface and bottom salinity from a mooring site in 20 m of water on the Alabama shelf are analyzed in conjunction with a series of across-shelf CTD surveys to examine their variability. While small sample sizes limit the statistical significance of the data patterns, the temperature data contain a strong annual signal with little year to year variability throughout the water column, whereas the salinity data have a weak annual signal with large year to year and vertical variability. As a result, the density data have a relatively strong annual signal with some year to year variability, demonstrating the importance of both temperature and salinity at this coastal mooring location.

Seasonal mean vertical profiles from the time series data show different characteristics between the summer and winter at the mooring site. Seasonal mean across-shelf transects from the CTD data reveal three distinct regions with different seasonal characteristics. In lower Mobile Bay, the estuarine section of the transect, vertical temperature, and salinity gradients are present during both the winter and summer. At the opposite end of the transect over the shelf region, the gradient structure changes with season having vertical gradients during the summer and horizontal gradients during the winter. The region between Mobile Bay and station CP acts as a transition zone, blending the characteristics of the estuary and shelf regions.

For the relationships with the forcing functions, the low frequency salinity signal is correlated with river discharge, but the relationship is absent during the periods with unusually low discharge. At shorter synoptic time scales, both the estuarine response to the across-shelf wind stress and the shelf response to the along-shelf wind stress are significantly correlated with temperature/salinity variability. The estuarine response is important for the surface layer during the winter periods with strong across-shelf gradients in temperature/salinity. The shelf response resulting from Ekman dynamics is important for the bottom layer during both the winter and summer periods.

The influence of Mobile Bay is observed at all time scales examined in this study, emphasizing the estuarine influence on the Alabama shelf. River discharge and wind in both the across- and along-shelf directions are important forcing functions determining the estuarine–shelf exchanges, which in turn are found to contribute to the setting of the shelf hydrographic structure.

These mechanisms that influence the water column structure have ramifications on the physical transport of estuarine-derived nutrients, suspended material, and marine organisms.

Acknowledgements

This work would not have been possible without the collecting and archiving of the data by the Tech Support Group at the Dauphin Island Sea Lab, including Kyle Weis, Roxanne Robertson, Alan Gunter, Mike Dardeau, and Laura Linn. This work was supported by the Fisheries Oceanography in Coastal Alabama funded by Alabama Department of Conservation and Natural Resources—Marine Resources Division. A partial support for H.K. Ha was from KOPRI Grant (PE10260). Finally, we thank Rich Pawlowicz at the University of British Columbia for the freely available MATLAB *m_map* toolbox which we have found to be useful in our analysis of geophysical data.

References

Abston, J.R., Dinnel, S.P., Schroeder, W.W., Shultz, A.W., Wiseman Jr., W.J., 1987. Coastal sediment plume morphology and its relationship to environmental forcing: Main Pass, Mobile Bay, Alabama. In: Kraus, N.C. (Ed.), Coastal Sediments '87, vol. II. ASCE, New York, NY, pp. 1989–2005.

Bochdansky, A.B., Bollens, S.M., 2009. Thin layer formation during runaway stratification in the tidally dynamic San Francisco Estuary. Journal of Plankton Research 31, 1385–1390.

Cochrane, J.D., Kelly, F.J., 1986. Low-frequency circulation on the Texas–Louisiana continental shelf. Journal of Geophysical Research 91, 10645–10659.

Cushing, D.H., 1990. Plankton production and year—class strength in fish populations: An update of the match/mismatch hypothesis. In: Blaxter, J.H.S., Southward, A.J (Eds.), Advances in Marine Biology. Academic Press, San Diego, CA, pp. 250–313.

Dinnel, S.P., Wiseman Jr., W.J., 1986. Fresh water on the Louisiana and Texas shelf. Continental Shelf Research 6, 765–784.

Dinnel, S.P., Schroeder, W.W., Wiseman Jr., W.J., 1990. Estuarine–shelf exchange using Landsat images of discharge plumes. Journal of Coastal Research 6, 789–799.

Dzwonkowski, B., Park, K., 2010. Influence of wind stress and discharge on the mean and seasonal currents on the Alabama shelf of the northeastern Gulf of Mexico. Journal of Geophysical Research 115, C12052. doi:10.1029/2010JC006449.

Garvine, R.W., 2004. The vertical structure and subtidal dynamics of the inner shelf off New Jersey. Journal of Marine Research 62, 337–371.

He, R., Weisberg, R.H., 2002. West Florida shelf circulation and temperature budget for the 1999 spring transition. Continental Shelf Research 22, 719–748.

He, R., Weisberg, R.H., 2003. West Florida shelf circulation and temperature budget for the 1998 fall transition. Continental Shelf Research 23, 777–800. doi:10.1016/S0278-4343(03)00028-1.

Huh, O.K., Rouse Jr., L.J., Walker, N.D., 1984. Cold-air outbreaks over the northwest Florida continental shelf: Heat flux processes and hydrographic changes. Journal of Geophysical Research 89, 717–726.

Jochens, A.E., DiMarco, S.F., Nowlin W.D., Jr., Reid, R.O., Kennicutt, M.C., II, 2002. Northeastern Gulf of Mexico Chemical Oceanography and Hydrography Study: Synthesis Report. U.S. Department of the Interior, Minerals Management Service, Gulf of Mexico OCS Region, New Orleans, LA, OCS study MMS 2002-055, 586 p.

Kirincich, A.R., Barth, J.A., Grantham, B.A., Menge, B.A., Lubchenco, J., 2005. Wind-driven inner-shelf circulation off central Oregon during summer. Journal of Geophysical Research 110, C10S03. doi:10.1029/2004JC002611.

Large, W.G., Pond, S., 1981. Open ocean momentum flux measurements in moderate to strong winds. Journal of Physical Oceanography 11, 324–336.

Lentz, S.J., 2001. The influence of stratification on the wind-driven cross-shelf circulation over the North Carolina shelf. Journal of Physical Oceanography 31, 2749–2760.

Liu, Y., Weisberg, R.H., He, R., 2006. Sea surface temperature patterns on the West Florida Shelf using growing hierarchical self-organizing maps. Journal of Atmospheric & Oceanic Technology 23, 325–338.

Mackas, D.L., Batten, S., Trudel, M., 2007. Effects on zooplankton of a warmer ocean: Recent evidence from the Northeast Pacific. Progress in Oceanography 75, 223–252.

Morey, S.L., Martin, P.J., O'Brien, J.J., Wallcraft, A.A., Zavala-Hidalgo, J., 2003a. Export pathways for river discharged fresh water in the northern Gulf of Mexico. Journal of Geophysical Research 108, 3303. doi:10.1029/2002JC001674.

Morey, S.L., Schroeder, W.W., O'Brien, J.J., Zavala-Hidalgo, J., 2003b. The annual cycle of riverine influence in the eastern Gulf of Mexico basin. Geophysical Research Letters 30, 1867. doi:10.1029/2003GL017348.

Morey, S.L., Zavala-Hidalgo, J., O'Brien, J.J., 2005. The seasonal variability of continental shelf circulation in the northern and western Gulf of Mexico from a high-resolution numerical model. In: Sturges, W., Lugo-Fernandez, A. (Eds.), Circulation in the Gulf of Mexico: Observations and Models, Geophysical Monograph Series 161. AGU, Washington, DC, pp. 203–218. doi:10.1029/161GM16.

Morey, S.L., Dukhovskoy, D.S., Bourassa, M.A., 2009. Connectivity of the Apalachicola River flow variability and the physical and bio-optical oceanic properties of the northern West Florida Shelf. Continental Shelf Research 29, 1264–1275. doi:10.1016/j.csr.2009.02.003.

Münchow, A., Chant, R.J., 2000. Kinematics of inner shelf motions during the summer stratified season off New Jersey. Journal of Physical Oceanography 30, 247–268.

Park, K., Kim, C.-K., Schroeder, W.W., 2007. Temporal variability in summertime bottom hypoxia in shallow areas of Mobile Bay, Alabama. Estuaries and Coasts 30, 54–65.

Sanders, T.M, Garvine, R.W., 2001. Fresh water delivery to the continental shelf and subsequent mixing: An observational study. Journal of Geophysical Research 106, 27087–27101.

Schroeder, W.W., 1979. The dispersion and impact of Mobile River system waters in Mobile Bay, Alabama. Bulletin 37. Water Resources Research Institute, Auburn University, Auburn, AL, 48 p.

Schroeder, W.W., Wiseman, W.J., Jr., 1985. An analysis of the winds (1974–1984) and sea level elevations (1973–1983) in coastal Alabama. Publication no. MASGP-84-024, Mississippi-Alabama Sea Grant Consortium, 102 p.

Schroeder, W.W., Wiseman Jr., W.J., 1986. Low-frequency shelf–estuarine exchange processes in Mobile Bay and other estuarine systems on the northern Gulf of Mexico. In: Wolfe, D.A. (Ed.), Estuarine Variability. Academic Press, New York, NY, pp. 355–366.

Stumpf, R.P., Gelfenbaum, G., Pennock, J.R., 1993. Wind and tidal forcing of a buoyant plume, Mobile Bay, Alabama. Continental Shelf Research 13, 1281–1301.

Sverdrup, H.U., 1953. On conditions for the vernal blooming of phytoplankton. Journal du Conseil, Conseil International pour l'Exploration de la Mer 18, 287–295.

Turner, R.E., Schroeder, W.W., Wiseman Jr., W.J., 1987. The role of stratification in the deoxygenation of Mobile Bay adjacent shelf bottom waters. Estuaries 10, 13–19.

Virmani, J.I., Weisberg, R.H., 2003. Features of the observed annual ocean–atmosphere flux variability on the West Florida Shelf. Journal of Climate 16, 734–745.

Weisberg, R.H., Black, B.D., Li, Z., 2000. An upwelling case study on Florida's west coast. Journal of Geophysical Research 105, 11459–11469.

Weisberg, R.H., Li, Z., Muller-Karger, F.E., 2001. West Florida shelf response to local wind forcing: April 1998. Journal of Geophysical Research 106, 31239–31262.

Weisberg, R.H., He, R., 2003. Local and deep-ocean forcing contributions to anomalous water properties on the West Florida Shelf. Journal of Geophysical Research 108, 3184. doi:10.1029/2002JC001407.

Wiseman, Jr., W.J., Schroeder, W.W, Dinnel, S.P., 1988. Shelf-estuarine water exchanges between the Gulf of Mexico and Mobile Bay, Alabama. American Fisheries Society Symposium 3, 1–8.

Wiseman Jr., W.J., Kelly, F.J., 1994. Salinity variability within the Louisiana coastal current during the 1982 flood season. Estuaries 17, 732–739.

Wiseman, W.J., Rabalais, N.N., Turner, R.E., Dinnel, S.P., MacNaughton, A., 1997. Seasonal and interannual variability within the Louisiana coastal current: Stratification and hypoxia. Journal of Marine Systems 12, 237–248.